QUARTERLY JOURNAL OF THE ROYAL METEOROLOGICAL SOCIETY
Q. J. R. Meteorol. Soc. **133**: 2109–2115 (2007)
Published online in Wiley InterScience
(www.interscience.wiley.com) DOI: 10.1002/qj.171

RMetS
ROYAL METEOROLOGICAL SOCIETY

Winter jet stream trends over the Northern Hemisphere

Courtenay Strong[a]* and Robert E. Davis[b]
[a] *University of California, Irvine, USA*
[b] *Department of Environmental Sciences, University of Virginia, Charlottesville, USA*

ABSTRACT: Trends in the speed and probability of winter jet stream cores over the Northern Hemisphere were measured for 1958–2007, and related changes in the thermal structure of the troposphere were identified. Eddy-driven jet (EDJ) core speeds and probabilities increased over the midlatitudes (40–60 °N), with changes as large as 15% (speed) and 30% (probability). These increasing trends are collocated with increases in baroclinicity driven by a spatially heterogeneous pattern of height change consisting of large-scale warming with cooling centres embedded poleward of 60 °N. The cooling centres reduced high-latitude baroclinicity, making jet cores poleward of 60 °N less frequent and weaker. Over the west and central Pacific, subtropical jet stream (STJ) core probabilities remained relatively constant while core speeds increased by as much as 1.75 m/s decade^{-1} in association with Hadley cell intensification. The STJ shifted poleward over the east Pacific and Middle East, and an equatorward shift and intensification of the STJ were found over the Atlantic basin–contributing to an increased separation of the EDJ and STJ. Copyright © 2007 Royal Meteorological Society

KEY WORDS general circulation; climate change; global warming

Received 25 March 2007; Revised 23 August 2007; Accepted 18 September 2007

1. Introduction

Modest changes in the jet stream's position and strength can impact midlatitude storm tracks (Nakamura, 1992), severe weather (Kloth and Davies-Jones, 1980), stratosphere–troposphere exchange (Wei, 1987), and circulation regimes (Ruti *et al*., 2006). Given the jet stream's sensitivity to the distribution of air temperature (e.g. Palmén, 1948), jet stream variability will likely be affected by climate change and the evolving thermal structure of the troposphere. Projections by fifteen coupled global climate models predict intensification and poleward shifts in 21st-century storm tracks, implying poleward shifts in the jet streams of both hemispheres (Yin, 2005).

Patterns observed in the historical record include poleward trends in surface cyclone frequency (McCabe *et al*., 2001), contracting and strengthening of the circumpolar vortex since 1970 (Frauenfeld and Davis, 2003), increasing strength of the winter Hadley circulation since the 1950's (Mitas and Clement, 2005), and an approximately one-degree poleward shift in the position of tropospheric jet streams during 1979–2005 implied by satellite-derived radiances (Fu *et al*., 2006).

The pattern of tropospheric temperature trends over the Northern Hemisphere is spatially heterogeneous. Regional, high-latitude pockets of decreasing temperature are embedded within a larger-scale pattern of increasing temperature. The spatial configuration of the temperature trends can be related to the spatial patterns of the atmosphere's leading modes of internal variability (Wu and Straus, 2004), in accord with modelling and observational studies suggesting that the atmosphere's response to enhanced radiative forcing may largely project onto leading patterns of internal variability (Corti *et al*., 1999; Fyfe *et al*., 1999; Palmer, 1999; Stone *et al*., 2001 and references therein). Wu and Straus (2004) showed that much of the winter tropospheric height, pressure and temperature trends over the Euro-Atlantic area project onto the Arctic Oscillation (AO) (Thompson and Wallace, 2000), while those over the Pacific–North American sector project onto the cold ocean–warm land (COWL) pattern (Wallace *et al*., 1996; Hsu and Zwiers, 2001). COWL is related to the difference in thermal inertia between land and ocean (Broccoli *et al*., 1998; Lu *et al*., 2004) and has an upper tropospheric signature resembling elements of the Pacific–North American (PNA) pattern (Lu *et al*., 2004; Wu and Straus, 2004).

Although mean properties of winter jet streams have been analysed in the context of temperature over the Northern Hemisphere (Koch *et al*., 2006; Strong and Davis, 2006a), jet core trends have yet to be assessed. Here, we measure the probability and speed of upper tropospheric jet stream cores over the Northern Hemisphere for winters 1958 to 2007, test for jet core trends, and identify the related tropospheric thermal structure changes.

2. Data and methods

2.1. Data and statistical methods

From the NCEP–NCAR Reanalysis (Kalnay *et al*., 1996), we use six-hourly December–February (DJF)

* Correspondence to: Courtenay Strong, University of California, Croul Hall, Irvine, CA 92697, USA. E-mail: cstrong@uci.edu

lapse-rate tropopause pressure and isobaric air temperature, wind velocity, and geopotential height (Z), each at 2.5° resolution. The ECMWF ERA-40 Reanalysis (Uppala *et al*., 2005) has some documented differences from the NCEP–NCAR Reanalysis over the midlatitudes during winter (Dell'Aquila *et al*., 2005), so we repeat elements of our trend analysis using monthly mean Z from the ERA-40. Both datasets may contain inhomogeneities or discontinuities related to variations in assimilation, including the introduction of satellite data (e.g. Dell'Aquila *et al*., 2005). Much of the signal underlying the sense of the trends reported here, however, is associated with changes in the post-satellite era. For example, more than 98% of the area shaded with significant 250 hPa Z trends for 1958–2007 (to be shown in section 3, Figure 4(a)) has like-signed trends for the 1979–2007 period, with more than half the trend area retaining significance despite the reduced degrees of freedom.

For each reanalysis, winter circumpolar vortex data were developed using monthly mean 300 hPa Z following Frauenfeld and Davis (2003), and the winter mean vortex position at each meridian was obtained by averaging the DJF values for each year. The circumpolar vortex is a useful diagnostic because it represents, in one variable, the size, strength, shape and Rossby-wave structure of the tropospheric circulation. The strength of the Hadley circulation is calculated as the DJF mean of the maximum value of the stream function of the meridional overturning circulation from 0° to 30 °N following Oort and Yienger (1996).

Trends are first examined for statistical significance using a parametric method that accounts for serial correlation by using a t-test with effective degrees of freedom

$$\upsilon = (n-1)(1-\rho)/(1+\rho), \tag{1}$$

where n is the sample size and ρ is the lag-1 autocorrelation in the regression residuals (Wilks, 2005). For regions where the parametric test indicates a significant trend, we further check significance using a bootstrap method that accounts for serial correlation as described in detail by De Wet and Van Wyk (1986). Briefly, a first-order autoregressive (AR-1) model is developed for the regression residuals, a sampling distribution for the regression coefficient b is developed using 1000 time series generated by the slope estimate and bootstrapped errors of the AR-1 model, and the b distribution's quantiles are used to calculate confidence limits. The parametric method and bootstrap method are performed at the 95% confidence level, and trends reported as significant at $\alpha = 0.05$ have passed both tests.

2.2. The Surface of Maximum Wind

Wind speed data on a single isobaric surface (e.g. 250 hPa) are often used to represent the jet stream or to construct zonal wind indices, but such analyses may lead to inaccurate conclusions about jet stream variability since jet core pressures vary spatially and temporally. Temporal variations of jet core position relative to an isobaric surface can be of order 10^2 hPa (Strong and Davis, 2005), so an isobaric jet stream analysis may indicate false, or mask actual, variability patterns including trends. To circumvent these potential difficulties, we use the Surface of Maximum Wind (SMW) analysis frame as described in Strong and Davis (2005, 2006a, 2006b, 2007). At a given observation time the SMW is the quasi-horizontal surface that passes through the fastest wind in each column of the atmosphere with a vertical search domain restricted to the upper troposphere and any tropospheric jet streams extending into the lower stratosphere.

2.3. Jet core probability and speed

On the SMW, we define a jet core as a local maximum of wind speed greater than or equal to 25.7 m/s based on a second derivative test along each meridian. For any location, mean winter jet core speed ($\overline{V}_{\text{core}}$) is the SMW wind speed averaged over winter observation times when a jet core is present at the location, and jet core probability ($0 \leq \tilde{C} \leq 1$) is the relative frequency of jet core occurrence at the location (i.e. the fraction of winter observation times for which a jet core is present at the location).

3. Results

3.1. Jet core climatology

The belt of relatively high $\tilde{C}$ from 40 to 60 °N (shading, Figure 1(a)) reflects the frequent presence of eddy-driven jet stream (EDJ) cores. EDJ cores tend to have higher mean speeds ($\overline{V}_{\text{core}}$, Figure 1(b)) where they occur close to the baroclinicity of the circumpolar vortex (e.g. compare data at 30 °W 45 °N and 60 °E 60 °N in Figure 1(a) and (b)). The subtropical jet stream (STJ) has a three-wave structure that is out of phase with the circumpolar vortex (compare ridges and troughs of dash–dot and bold curves in Figure 1). STJ core probabilities and speeds are highest where the subtropical jet approaches the vortex: over the Middle East and at the east coasts of Asia and North America (Figure 1(a) and (b)).

3.2. Jet core trends

Winter jet core probabilities ($\tilde{C}$) and mean speeds ($\overline{V}_{\text{core}}$) have positive trends over much of the midlatitudes of the Northern Hemisphere (40–60 °N, Figure 2(a) and (b)). Poleward of the circumpolar vortex across North America, the Atlantic and Europe, trends are related primarily to the EDJ, and cumulative increases amount to as much as 15% of local mean speed and 30% of local mean probability. The increasing frequency and strength of EDJ cores is physically consistent with baroclinicity enhancement indicated by the collocated corridor of increasing geopotential height gradients ($|\nabla Z|$) (Figure 2(c)), and the increasing $|\nabla Z|$ is consistent with the circumpolar vortex's poleward trend toward the region of EDJ core

DOI: 10.1002/qj

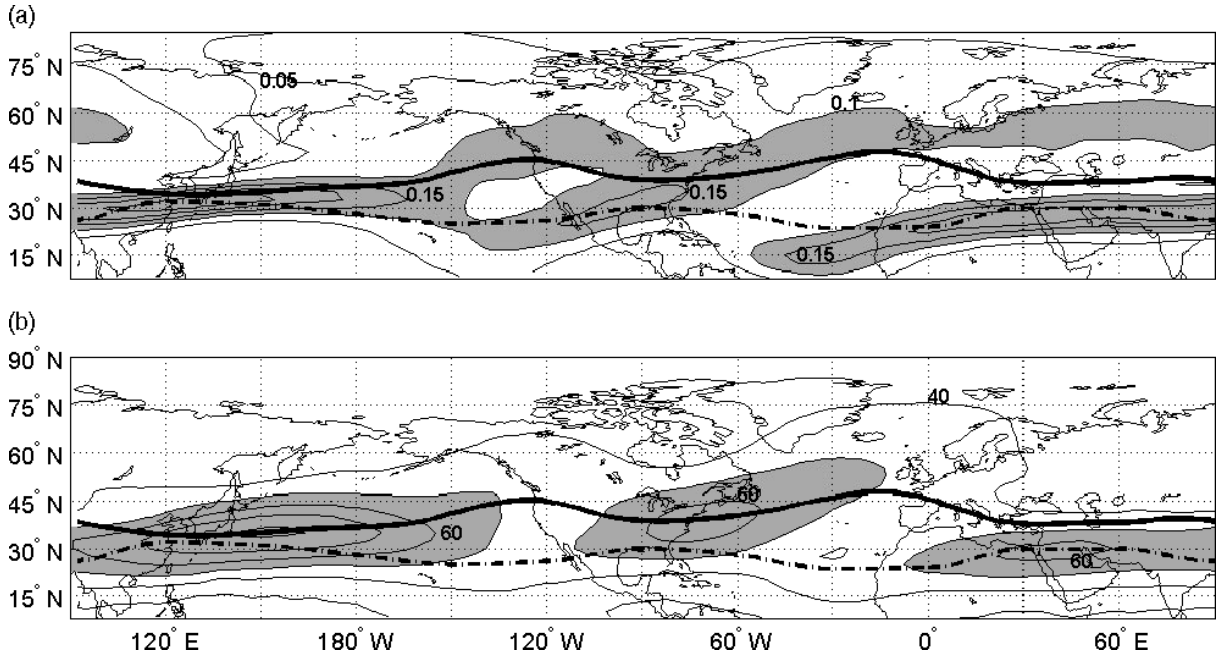

Figure 1. For winters 1958–2007: (a) jet core probability ($\tilde{C}$) contoured at 0.05 with values greater than 0.1 shaded and (b) mean jet core speed ($\overline{V}_{\text{core}}$) contoured at 10 m/s with values greater than 50 m/s shaded. The bold curve shows the mean position of the circumpolar vortex and the dash–dot curve shows the mean position of the subtropical jet stream adapted from Krishnamurti (1961).

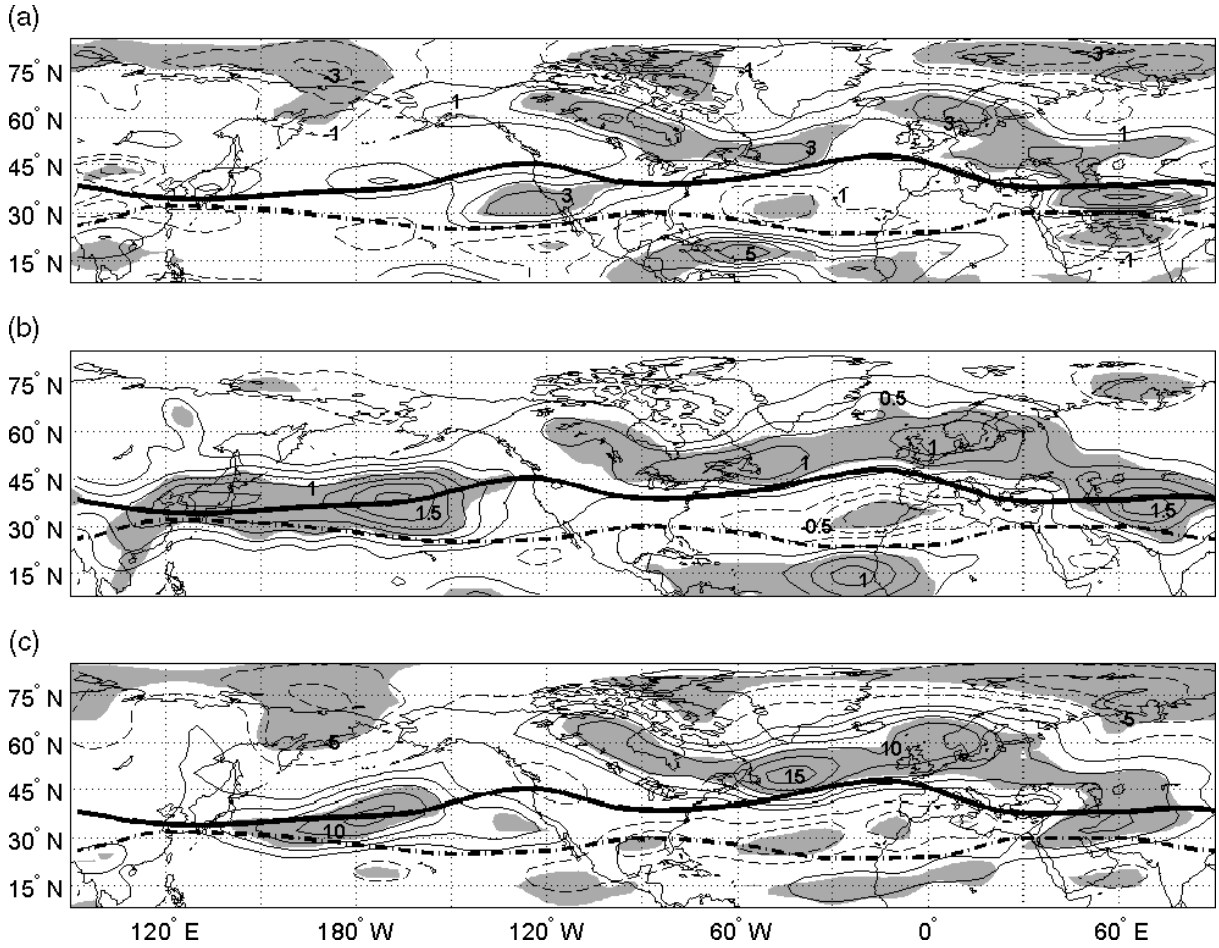

Figure 2. Trends for winters (DJF) 1958–2007: (a) jet core probability ($\tilde{C}$) contoured at 10^{-3} decade^{-1}, (b) jet core speed ($\overline{V}_{\text{core}}$) contoured at 0.25 m/s decade^{-1}, and (c) geopotential height gradient ($|\nabla Z|$) contoured at 10^{-6} decade^{-1}. For all panels, negative values are dashed, the zero contour is suppressed, shading indicates significance at $\alpha = 0.05$, and the vortex (bold curve) and subtropical jet stream (dash–dot curve) are from Figure 1.

DOI: 10.1002/qj

intensification (arrows, Figure 3(b)). The declining $\tilde{C}$ and $\overline{V}_{\text{core}}$ trends poleward of 70 °N (Figure 2(a) and (b)) are associated with a decline in overall baroclinicity across the high latitudes (Figure 2(c)).

Jet core trends along and south of the circumpolar vortex are related primarily to the STJ. Across much of the Pacific STJ, winter $\overline{V}_{\text{core}}$ has been increasing by up to 1.75 m/s decade^{-1} (along 35 °N, Figure 2(b)). Much of this increase is accounted for by the increasing strength of the Hadley circulation, as indicated by the correlation analysis in Figure 3(a). Detailed linkage between the Hadley circulation and atmospheric temperature is given in, for example, Quan *et al*. (2004). The relative lack of $\tilde{C}$-changes along the midlatitudes of the Pacific reflects the persistence and positional stability of the Pacific STJ ($\tilde{C}$ as large as 0.25, Figure 1(a)).

The STJ is trending equatorward over the Atlantic near 60 °W and poleward over the Middle East and east Pacific; shifts in the position of the STJ are indicated by $\tilde{C}$ trend dipoles flanking the dash-dot curve in Figure 2(a), and there is a logical sign relationship between the $\tilde{C}$ trend dipoles and $|\nabla Z|$ trends (Figure 2(a) and (c)). These poleward and equatorward STJ shifts are influenced by a positive trend in the strength of the Hadley circulation (Figure 3(a), $\tilde{C}$ correlation with Hadley circulation not shown). The STJ's equatorward trend over the Atlantic is also related to a tendency for poleward vortex trends to separate the EDJ and STJ over the Atlantic basin (correlation tripole over east Atlantic, Figure 3(b)).

3.3. Tropospheric thermal structure

We now examine the tropospheric temperature and Z changes underlying the reported jet core trends, and compare Z trend results in the NCEP Reanalysis (Figure 4(a)) with those in the ERA-40 (Figure 4(b)). The height trends (which suggest temperature trends via the hypsometric relationship) are spatially heterogeneous, featuring large-scale height increases over much of the Tropics and midlatitudes, and centres of decreasing height poleward of 60 °N. The cooling poleward of warming accounts for the enhanced (weakened) baroclinicity over the midlatitudes (high latitudes), and the observed winter $\overline{V}_{\text{core}}$ trends are in approximate geostrophic balance with the height changes. As a quantitative example, the maximum jet core speed trend along 180° is 1.72 m/s decade^{-1}. The collocated $\partial Z/\partial y$ trend of 1.39×10^{-5} decade^{-1} indicates a 1.74 m/s decade^{-1} trend in the geostrophic zonal wind.

The centres of increasing Z are consistent (location and magnitude) between the NCEP Reanalysis and ERA-40, although the NCEP significance is spatially broader over western Canada and the equatorial Atlantic. In the ERA-40 data, the high-latitude Z decreases are generally stronger and have more spatially broad significance than in the NCEP data, particularly from 0° to 90 °W, implying stronger $\overline{V}_{\text{core}}$ trends in the ERA-40. For both datasets, the vortex contracts where it encounters significant positive height trends (i.e. the arrow bases are collocated with shading, Figure 4). The vortex is related to air temperature as further described in Frauenfeld and Davis (2003).

We now use cross-sectional data from 180° to illustrate how the relevant changes in the thermal structure of the troposphere are configured relative to the SMW (Figure 5). The cross-section reveals a tripole of $\partial Z/\partial y$ trends each of which is centred near the SMW (along bold curve near 15, 30 and 70 °N, Figure 5(a)). The two northernmost $\partial Z/\partial y$ trends pair logically with core speed trends seen on the SMW (Figure 2(a) and (b)), whereas the equatorward $\partial Z/\partial y$ trend is occurring in a region where wind speeds rarely achieve jet core

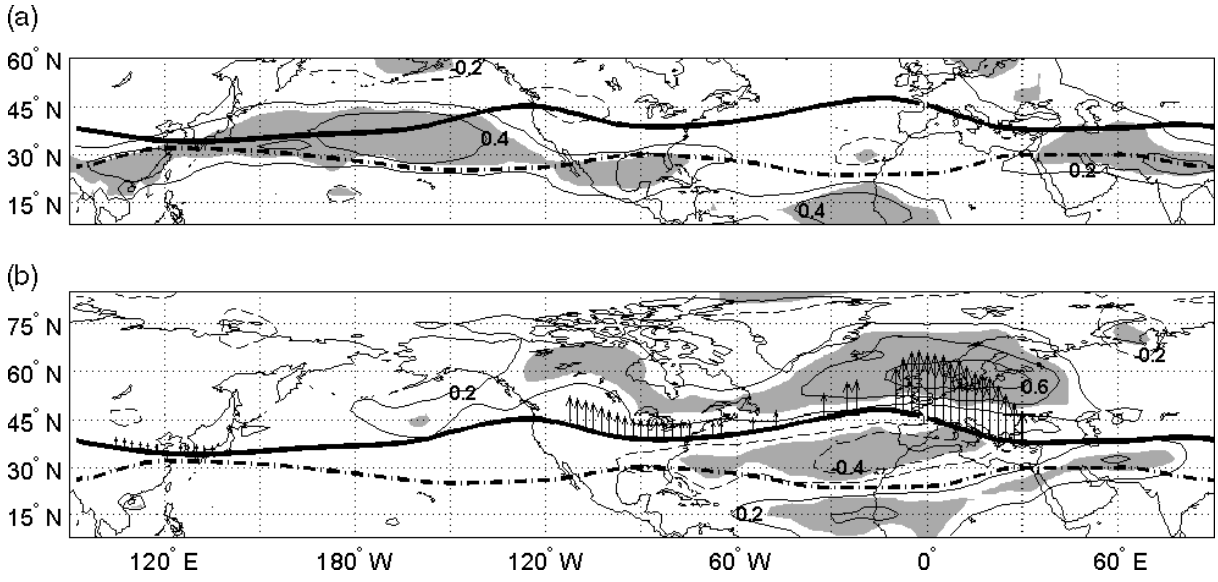

Figure 3. (a) Correlation between $\overline{V}_{\text{core}}$ and the strength of the Hadley circulation. (b) Arrows show the direction and magnitude of circumpolar vortex trends significant at $\alpha = 0.05$, where the longest arrow indicates 1.19° decade^{-1}. Contours show correlation between $\overline{V}_{\text{core}}$ and the vortex averaged over the meridians with arrows. For both panels, contouring and shading conventions follow Figure 2.

DOI: 10.1002/qj

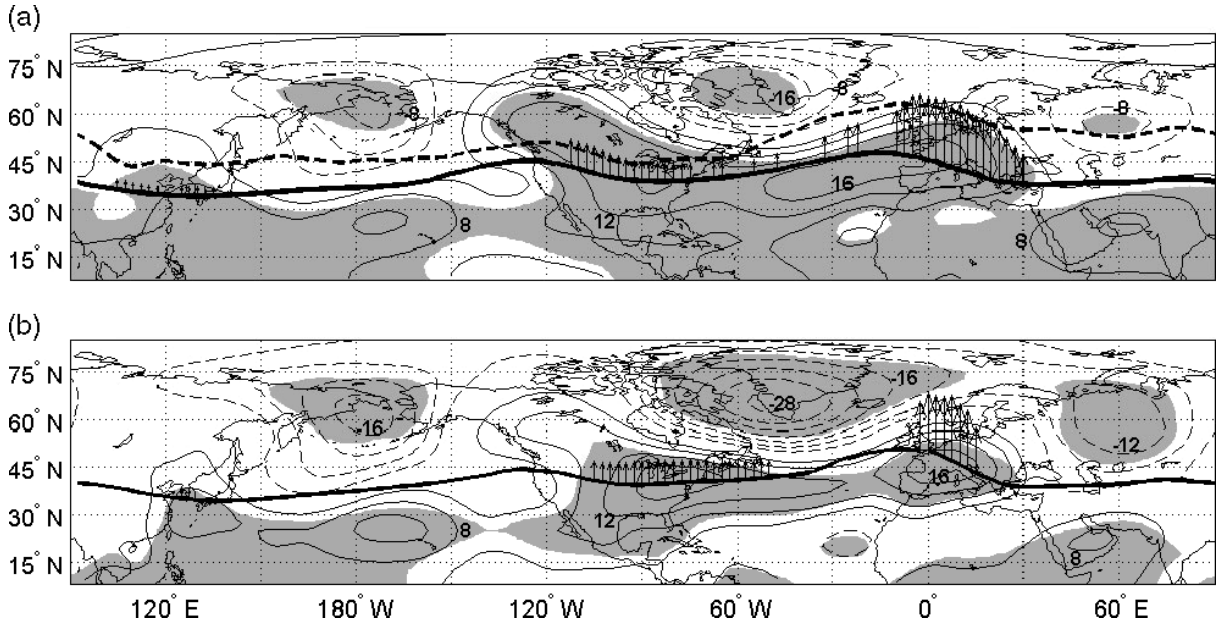

Figure 4. (a) For winters (DJF) 1958–2007, the trend in mean 250 hPa Z contoured at 4 m decade^{-1}. (b) Same as (a), but using ERA-40 data. For both panels, contouring and shading conventions follow Figure 2 and arrows follow Figure 3(b).

strength (Figure 1(a) and (b)). The $\partial Z/\partial y$ trends are associated with three height trends of logical sign and configuration that extend through a substantial depth of the troposphere and lower stratosphere (Figure 5(b)). The three regional temperature trends underlying the height trends are at a maximum approximately 100 hPa below the SMW (below bold curve near 25, 65 and 90 °N, Figure 5(c)). For other meridians, similar logical relationships are found between the isobaric height trends shown in Figure 4(a) and cross-sectional trends in the thermal structure of the underlying troposphere (not shown).

4. Summary and discussion

We used the surface of maximum wind (SMW) analysis frame to directly measure jet stream core probability and speed trends over the Northern Hemisphere for 1958–2007, and identified related changes in the thermal structure of the troposphere. The pressure of the SMW analysis frame changes to coincide with the fastest observed wind speeds in each column of the upper troposphere and lower stratosphere, yielding more accurate jet core statistics than analyses based on a single isobaric surface, since jet core pressure variability relative to an isobaric analysis frame can generate false, or mask actual, variability patterns including trends.

EDJ core speeds and probabilities increased over the midlatitudes (40–60 °N), with changes as large as 15% (speed) and 30% (probability). These increasing trends are collocated with increases in baroclinicity driven by a spatially heterogeneous pattern of height change consisting of large-scale warming with cooling centres embedded poleward of 60 °N. The cooling centres reduced baroclinicity poleward of 60 °N, making jet cores less frequent and weaker over the polar latitudes. Over the west and central Pacific, STJ core probabilities remained relatively constant while core speeds increased by as much as 1.75 m/s decade^{-1} in association with enhanced poleward transport of angular momentum in the Hadley circulation. The STJ shifted poleward over the east Pacific and Middle East, and an equatorward shift and intensification of the Atlantic STJ were found over the Atlantic basin – contributing to an increased separation of the EDJ and STJ.

Considering the $\overline{V}_{\text{core}}$ and $\tilde{C}$ trend results together, the EDJ's high-latitude intensification and separation from the STJ over the Euro-Atlantic area resemble aspects of the jet core response to the positive polarity of the AO, and the intensification or eastward expansion of the Pacific STJ resemble aspects of the jet core response to the PNA pattern or COWL (Strong and Davis, 2007). The presence of these similarities is consistent with research showing that portions of the height trends over these sectors have thermal structures that project onto, respectively, the spatial patterns of the AO and COWL (Wu and Straus, 2004), but should not be taken to imply an absence of anthropogenic forcing (Corti *et al*., 1999; Fyfe *et al*., 1999; Palmer, 1999; Stone *et al*., 2001 and references therein).

The reported jet stream trends are largely in geostrophic balance with thermal changes in the troposphere on a seasonal mean basis. Nonetheless, changes in jet stream position and intensity can feed back onto the spatial distribution of temperature in the atmosphere by inducing transverse vertical circulations or altering the spatial patterns of cloudiness, latent heating and precipitation. If the atmosphere's response to radiative forcing by greenhouse gases were more uniform, $\tilde{C}$ and $\overline{V}_{\text{core}}$ trends might be less pronounced, particularly within the EDJ,

DOI: 10.1002/qj

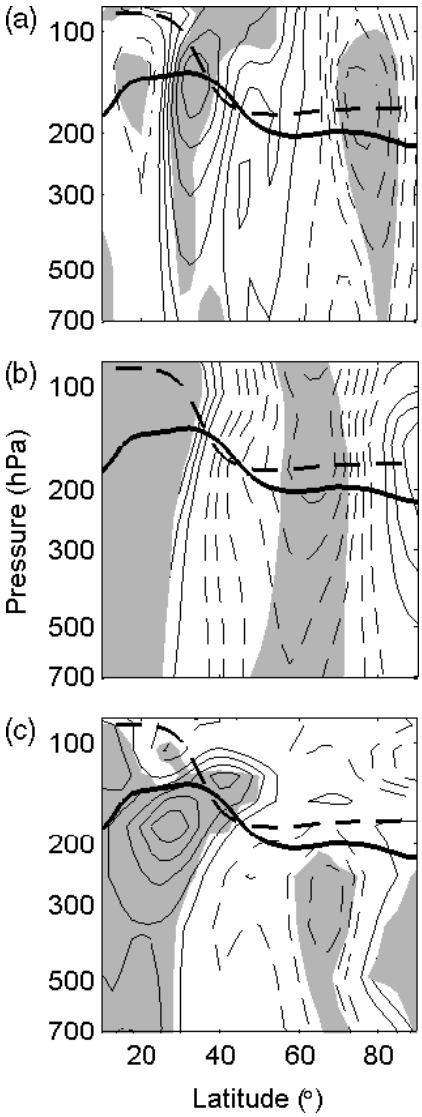

Figure 5. Trends for winters (DJF) 1958–2007 along 180°: (a) geopotential height gradient contoured at 4×10^{-6} decade^{-1}, (b) geopotential height contoured at 2 m decade^{-1}, and (c) air temperature contoured at 0.1 K decade^{-1}. In each panel, the bold solid curve is the mean surface of maximum wind (SMW), the bold dashed curve is the mean tropopause, and contouring and shading conventions follow Figure 2.

since the position and baroclinicity of the circumpolar vortex depend more on temperature gradients than on mean hemispheric temperature. Instead, the climate system's response to observed and projected increases in greenhouse gas concentrations features oppositely-signed temperature trends and shifts in baroclinicity as robust components. The spatial patterns of these trends can be related to the atmosphere's leading patterns of internal variability, providing evidence of the importance of understanding how such leading variability patterns will evolve under projected climate change.

Acknowledgements

NCEP–NCAR Reanalysis data were obtained from the NOAA Climate Diagnostics Center server and ECMWF ERA-40 data were obtained from the ECMWF online server. C. Strong was supported by a US National Science Foundation Graduate Research Fellowship. Excellent comments from two anonymous reviewers helped to improve the manuscript.

References

Broccoli AJ, Lau N-C, Nath MJ. 1998. The cold ocean–warm land pattern: Model simulation and relevance to climate change detection. *J. Climate* **11**: 2743–2763.

Corti S, Molteni F, Palmer TN. 1999. Signature of recent climate change in frequencies of natural atmospheric circulation regimes. *Nature* **398**: 799–802.

De Wet T, Van Wyk JWJ. 1986. Bootstrap confidence intervals for regression coefficients when the residuals are dependent. *J. Statist. Comput. Simul.* **23**: 317–327.

Dell'Aquila A, Lucarini V, Ruti PM, Calmanti S. 2005. Hayashi spectra of the northern hemisphere mid-latitude atmospheric variability in the NCEP–NCAR and ECMWF reanalyses. *Clim. Dyn.* **25**: 639–652.

Frauenfeld OW, Davis RE. 2003. Northern Hemisphere circumpolar vortex trends and climate change implications. *J. Geophys. Res.* **108**: 4423, doi: 10.1029/2002JD002958.

Fyfe JC, Boer GJ, Flato GM. 1999. The Arctic and Antarctic Oscillations and their projected changes under global warming. *Geophys. Res. Lett.* **26**: 1601–1604.

Fu Q, Johanson CM, Wallace JM, Reichler T. 2006. Enhanced mid-latitude tropospheric warming in satellite measurements. *Science* **312**: 1179, doi: 10.1126/science.1125566.

Hsu CJ, Zwiers F. 2001. Climate change in recurrent regimes and modes of Northern Hemisphere atmospheric variability. *J. Geophys. Res.* **106**: 20145–20159.

Kalnay E, Kanamitsu M, Kistler R, Collins W, Deaven D, Gandin L, Iredell M, Saha S, White G, Woollen J, Zhu Y, Leetma A, Reynolds B, Chelliah M, Ebisuzaki W, Higgins W, Janowiak J, Mo KC, Ropelewski C, Wang J, Jenne R, Joseph D. 1996. The NCEP/NCAR 40-year reanalysis project. *Bull. Am. Meteorol. Soc.* **77**: 437–471.

Kloth CM, Davies-Jones RP. 1980. 'The relationship of the 300-mb jet stream to tornado occurrence.' NOAA Technical Memorandum ERL NSSL-88.

Koch P, Wernli H, Davies HC. 2006. An event-based jet stream climatology and typology. *Int. J. Climatol.* **26**: 283–301.

Krishnamurti TN. 1961. The subtropical jet stream of winter. *J. Atmos. Sci.* **18**: 172–191.

Lu J, Greatbatch RJ, Peterson KA. 2004. Trend in Northern Hemisphere winter atmospheric circulation during the last half of the twentieth century. *J. Climate* **17**: 3745–3760.

McCabe GJ, Clark MP, Serreze MC. 2001. Trends in Northern Hemisphere surface cyclone frequency and intensity. *J. Climate* **14**: 2763–2768.

Mitas CM, Clement A. 2005. Has the Hadley cell been strengthening in recent decades? *Geophys. Res. Lett.* **32**: L03809, doi: 10.1029/2004GL021765.

Nakamura H. 1992. Midwinter suppression of baroclinic wave activity in the Pacific. *J. Atmos. Sci.* **49**: 1629–1642.

Palmén E. 1948. On the distribution of temperature and wind in the upper westerlies. *J. Meteorol.* **5**: 20–27.

Palmer TN. 1999. A nonlinear dynamical perspective on climate prediction. *J. Climate* **12**: 575–591.

Oort AH, Yienger JJ. 1996. Observed interannual variability in the Hadley circulation and its connection to ENSO. *J. Climate* **9**: 2751–2767.

Quan X-W, Diaz HF, Hoerling MP. 2004. Change in the tropical Hadley cell since 1950. Pp. 85–120 in *The Hadley circulation: Past, present, and future,* Diaz HF, Bradley RS (eds). Kluwer Academic Publishers.

Ruti PM, Lucarini V, Dell'Aquila A, Calmanti S, Speranza A. 2006. Does the subtropical jet catalyze the midlatitude atmospheric regimes? *Geophys. Res. Lett.* **33**: L06814, doi: 10.1029/2005GL024620.

Stone DA, Weaver AJ, Stouffer RJ. 2001. Projection of climate change onto modes of atmospheric variability. *J. Climate* **14**: 3551–3565.

Strong C, Davis RE. 2005. The surface of maximum wind as an alternative to the isobaric surface for wind climatology. *Geophys. Res. Lett.* **32**: L04813, doi: 10.1029/2004GL022039.

Strong C, Davis RE. 2006a. Variability in the altitude of fast upper tropospheric winds over the Northern Hemisphere during winter. *J. Geophys. Res.* **111**: D10106, doi: 10.1029/2005JD006497.

Strong C, Davis RE. 2006b. Temperature-related trends in the vertical position of the summer upper tropospheric surface of maximum wind over the Northern Hemisphere. *Int. J. Climatol.* **26**: 1977–1997.

Strong C, Davis RE. 2007. Variability in the position and strength of winter jet stream cores related to northern hemisphere teleconnections. *J. Climate,* in press.

Thompson DWJ, Wallace JM. 2000. Annular modes in the extratropical circulation. Part I: Month-to-month variability. *J. Climate* **13**: 1000–1016.

Uppala SM, Kållberg PW, Simmons AJ, Andrae U, da Costa Bechtold V, Fiorino M, Gibson JK, Haseler J, Hernandez A, Kelly GA, Li X, Onogi K, Saarinen S, Sokka N, Allan RP, Andersson E, Arpe K, Balmaseda MA, Beljaars ACM, van de Berg L, Bidlot J, Bormann N, Caires S, Chevallier F, Dethof A, Dragosavac M, Fisher M, Fuentes M, Hagemann S, Hólm E, Hoskins BJ, Isaksen L, Janssen PAEM, Jenne R, McNally AP, Mahfouf JF, Morcrette JJ, Rayner NA, Saunders RW, Simon P, Sterl A, Trenberth KE, Untch A, Vasiljević D, Viterbo P, Woollen J. 2005. The ERA-40 re-analysis. *Q. J. R. Meteorol. Soc.* **131**: 2961–3012.

Wallace JM, Zhang Y, Bajuk L. 1996. Interpretation of interdecadal trends in Northern Hemisphere surface air temperature. *J. Climate* **9**: 249–259.

Wei M-Y. 1987. A new formulation of the exchange of mass and trace constituents between the stratosphere and troposphere. *J. Atmos. Sci.* **44**: 3079–3086.

Wilks DS. 2005. *Statistical methods in the atmospheric sciences.* 2nd edition. International Geophysics Series, Volume 91. Academic Press.

Wu Q, Straus DM. 2004. AO, COWL, and observed climate trends. *J. Climate* **17**: 2139–2156.

Yin JH. 2005. A consistent poleward shift of the storm tracks in simulations of 21st century climate. *Geophys. Res. Lett.* **32**: L18701, doi: 10.1029/2005GL023684.